



Figures and figure supplements

Noncoding RNA-nucleated heterochromatin spreading is intrinsically labile and requires accessory elements for epigenetic stability

R A Greenstein et al

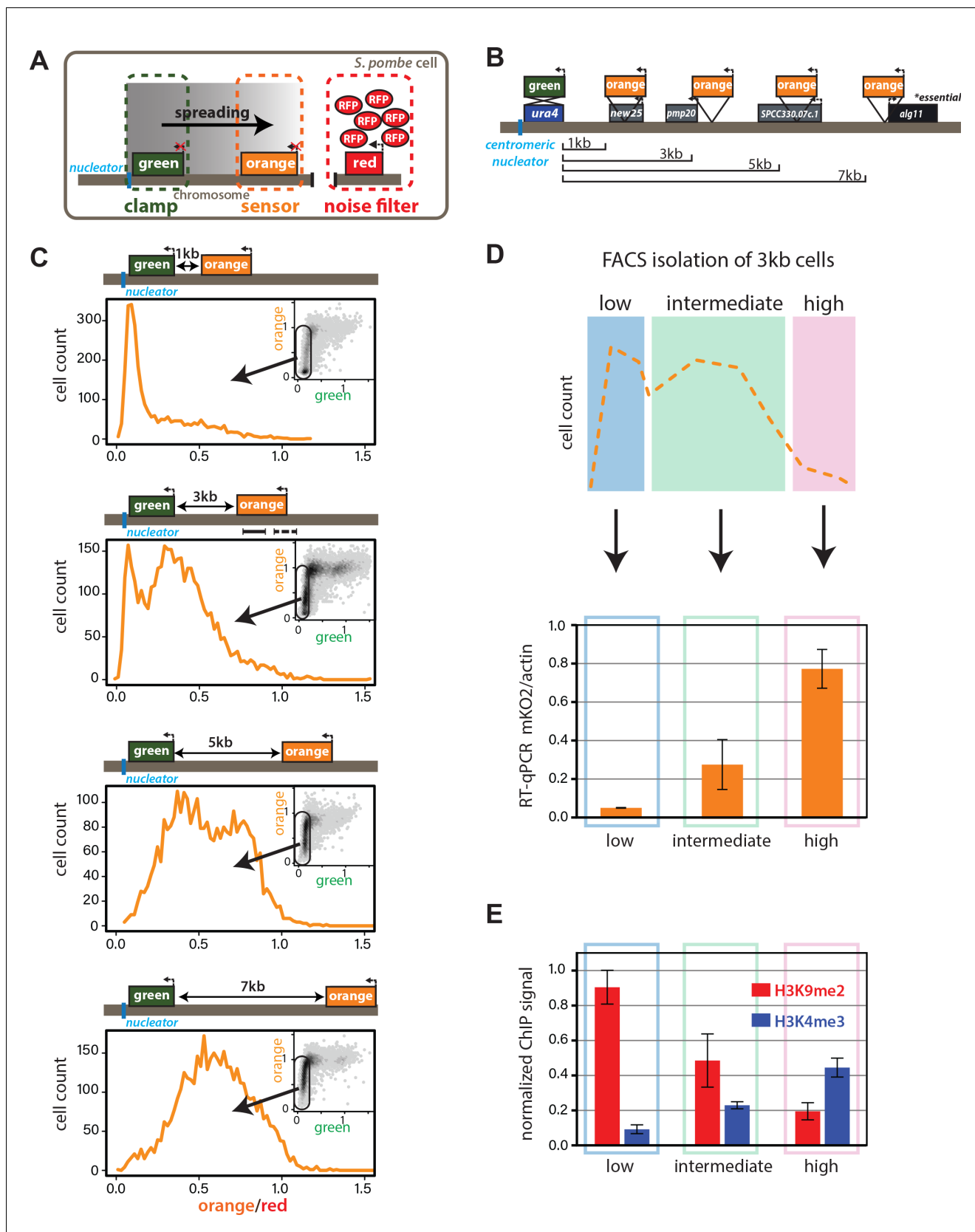


Figure 1. Heterochromatin spreading from ncRNA-nucleated elements is stochastic and produces intermediate states. (A) Overview of heterochromatin spreading sensor. Three transcriptionally encoded fluorescent proteins are inserted in the genome: The 'clamp' site enables isolation of cells where the nucleator has spread. (B) Genomic map showing the locations of the green, orange, and red genes relative to the *ura4* gene. (C) Cell count vs orange/red ratio for different distances (1kb, 3kb, 5kb, 7kb). (D) FACS isolation of 3kb cells. (E) RT-qPCR analysis of mRNA levels for *mKO2/actin* in the isolated groups. (F) ChIP signal analysis for H3K9me2 and H3K4me3 at the 3kb distance across low, intermediate, and high orange/red ratio groups.

Figure 1 continued

of successful nucleation events, the 'sensor' reports on spreading events and the 'noise filter' normalizes for cell-to-cell noise. (B) Overview of the *ura4::dhHSS^{1-7kb}* strains. Genes downstream of the 'green' nucleation color are annotated. The *alg11* gene is essential. (C) Spreading from *ura4::dh* visualized by the HSS with 'orange' inserted at different distances shown in (B). The 'red'-normalized 'orange' fluorescence distribution of 'green'^{OFF} cells plotted on a histogram. Inset: 2D-density hexbin plot showing red-normalized 'green' and 'orange' fluorescence within the size gate, with no 'green' or 'orange' filtering. The 'green'^{OFF} population is schematically circled. The fluorescence values are normalized to = 1 for the $\Delta clr4$ derivate of each strain. (D) TOP: cartoon overview of the FACS experiment for D. and E. 'green'^{OFF} cells collected from the *ura4::dhHSS^{3kb}* were separated in three populations ('Low', 'Intermediate' and 'High') as shown schematically based on the 'orange' fluorescence. BOTTOM: 'orange' RT-qPCR signal for the indicated populations. The y-axis is scaled to = 1 based on the 'orange' signal in $\Delta clr4$. Error bars indicate standard deviation of two replicate RNA isolations. (E) ChIP for H3K9me2 and H3K4me3 in the same populations as (D). Each ChIP is normalized over input and scaled to = 1 for a positive control locus (*dh* repeat for H3K9me2 and *act1* promoter for H3K4me3). Error bars indicate standard deviation of two technical ChIP replicates. Primer pairs for RT-qPCR and ChIP are indicated by solid and dashed line, respectively, in the C. *ura4::dhHSS^{3kb}* diagram.

DOI: <https://doi.org/10.7554/eLife.32948.002>

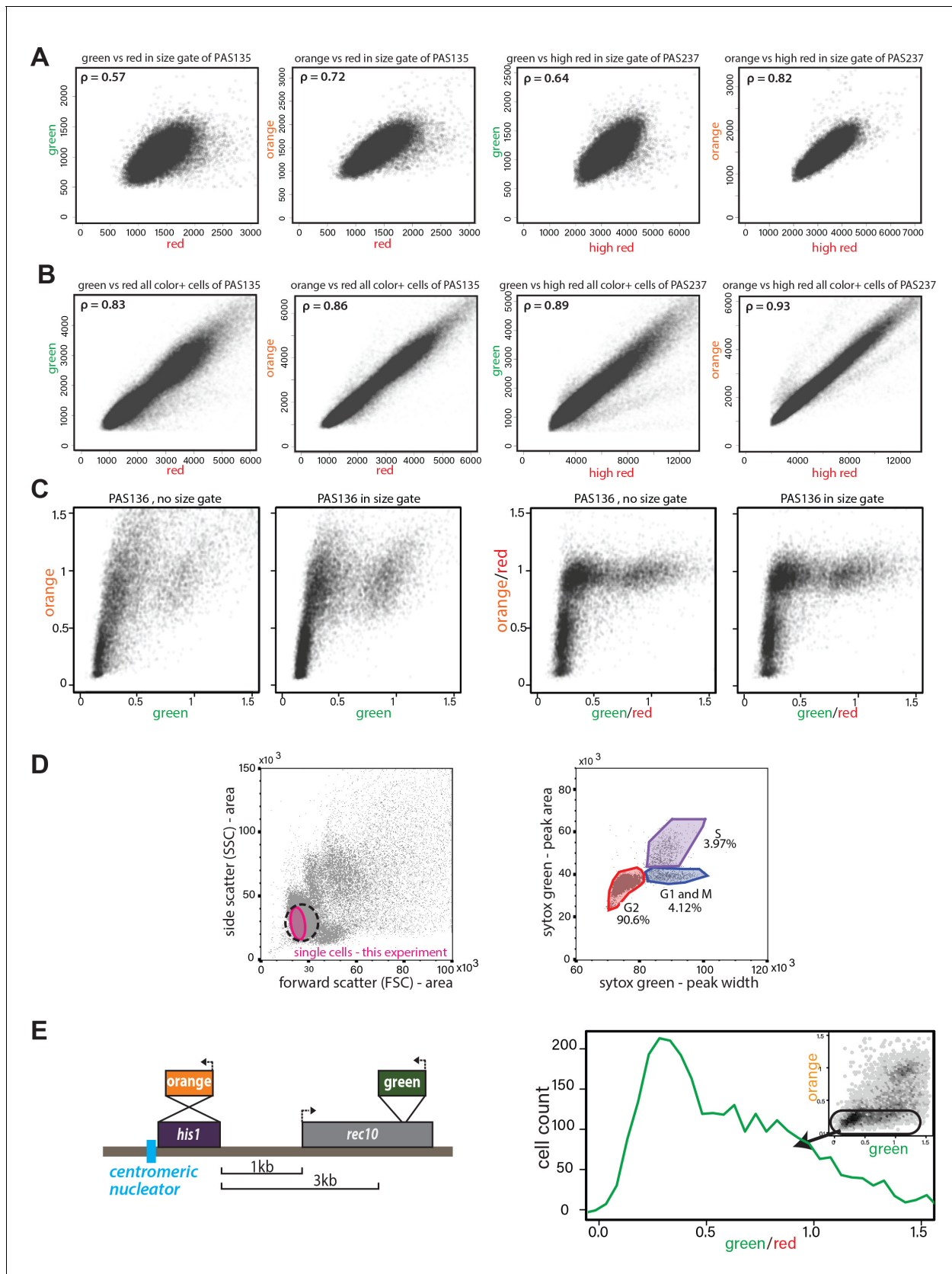


Figure 1—figure supplement 1. Validation of ectopic heterochromatin spreading sensor. (A) Correlation of *ade6p:SFGFP* or *ade6p:mKO2* with *ade6p:3XE2C* (Red) or *act1p:1XE2C* (High Red) in $\Delta clr4$ HSS size-gated cells. LEFT: Plots of green and orange vs. red channel signals of size-gated PAS Figure 1—figure supplement 1 continued on next page

Figure 1—figure supplement 1 continued

135 (Δ clr4, 'red'). RIGHT: Plots of green and orange vs. red channel signals of size-gated PAS 237 (Δ clr4, 'high-red'). The Pearson correlation between 'green' and 'red'/'high-red' or 'orange' and 'red'/'high-red' is shown. (B) Correlation of ade6p:SFGFP or ade6p:mKO2 with ade6p:3XE2C (Red) or act1p:1XE2C (High Red) in Δ clr4 HSS in cells without size gate. Plots and Pearson correlation as above. (C) Effect of red-normalization on distribution of clr4+ HSS cells. Plots of green and orange vs. red channel signals of PAS 136, which contains the ectopic HSS (Figure 1C). LEFT: effect of using only size gate, without red normalization. RIGHT: effect of red-normalization with and without additional size gate. The distribution of cells is tightened by red-normalization. (D) Cell cycle stage of HSS and wild-type cells by flow cytometry. Wild-type cells (PM03, see strain table) were fixed, stained with Sytox green DNA stain, and analyzed by flow cytometry. LEFT: side vs. forward scatter plot. Dotted line: The approximate size gate encompassing all experiments reported. Pink area: cells analyzed in the experiment shown. RIGHT: Plot of area vs. width parameter for the Sytox green channel, gates are drawn to denote cell cycle phases, G2 (red), G1 and M (Blue), S (purple) as described (Knutson et al., 2011). (E) Stochastic spreading and intermediate states produced by ncRNA-driven nucleators are replicated at a second ectopic site. LEFT: Overview of the his1::dhHSS^{3kb}. The colors are reversed relative to the ura4::dhHSS^{1-7kb} with 'orange' as the 'nucleation clamp' and 'green' as the 'sensor'. 'Orange' replaces the his1 gene and 'green' is located 3 kb downstream within the rec10 open-reading frame. RIGHT: histogram of 'red'-normalized 'green' fluorescence distribution of 'orange'^{OFF} cells. Inset: 2D density hexbin plot.

DOI: <https://doi.org/10.7554/eLife.32948.003>

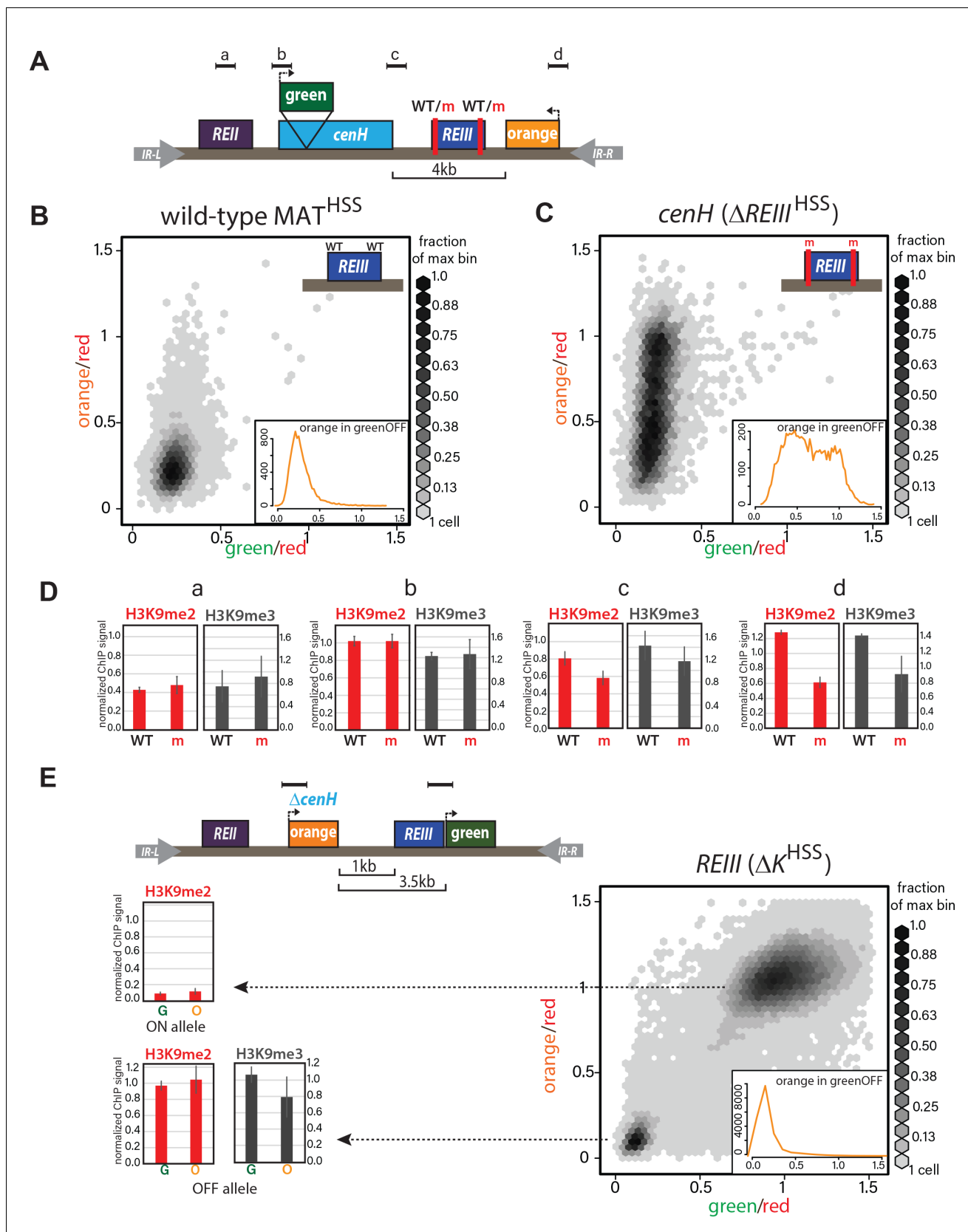


Figure 2. ncRNA-dependent and independent nucleation yields qualitatively different spreading reactions in the MAT locus. (A) Diagram of the reporters within MAT^{HSS} and $\Delta\text{REIII}^{\text{HSS}}$. WT and m for REIII indicate the presence or deletion of the Atf1/Pcr1 binding sites, respectively. (B) 2D-density Figure 2 continued on next page

Figure 2 continued

hexbin plot showing the 'red'-normalized 'green' and 'orange' fluorescence for wild-type MAT^{HSS} cells. Scale bar shows every other bin cutoff as a fraction of the bin with the most cells. Inset: histogram of the 'red'-normalized 'orange' fluorescence distribution of 'green'^{OFF} cells. (C) 2D-density hexbin plot and inset as above for $\Delta REIII^{HSS}$, which contains two 7 bp Atf1/Pcr1-binding site deletions (m) within the $REIII$ element. (D) ChIP for H3K9me2 (red) and H3K9me3 (grey) for amplicons indicated in (A), normalized to *dh*. WT, wild-type MAT^{HSS}, m, $\Delta REIII^{HSS}$. (E) TOP: diagram of the reporters within ΔK^{HSS} . The *cenH* nucleator and additional 5' sequence is deleted and replaced by 'orange'. 'green' is located directly proximal to $REIII$ and serves as the nucleation clamp. ChIP amplicons are indicated as black bars. BOTTOM: 2D-density hexbin plot and inset as above. LEFT: ChIP for H3K9me2 (red) and H3K9me3 (grey) for 'green' and 'orange' in isolated ΔK^{HSS-ON} or $\Delta K^{HSS-OFF}$ alleles. In hexbin plots, the $\Delta clr4$ derivative of each strain was used to normalize the X- and Y-axes to = 1. Error bars indicate standard deviation of technical replicates.

DOI: <https://doi.org/10.7554/eLife.32948.004>

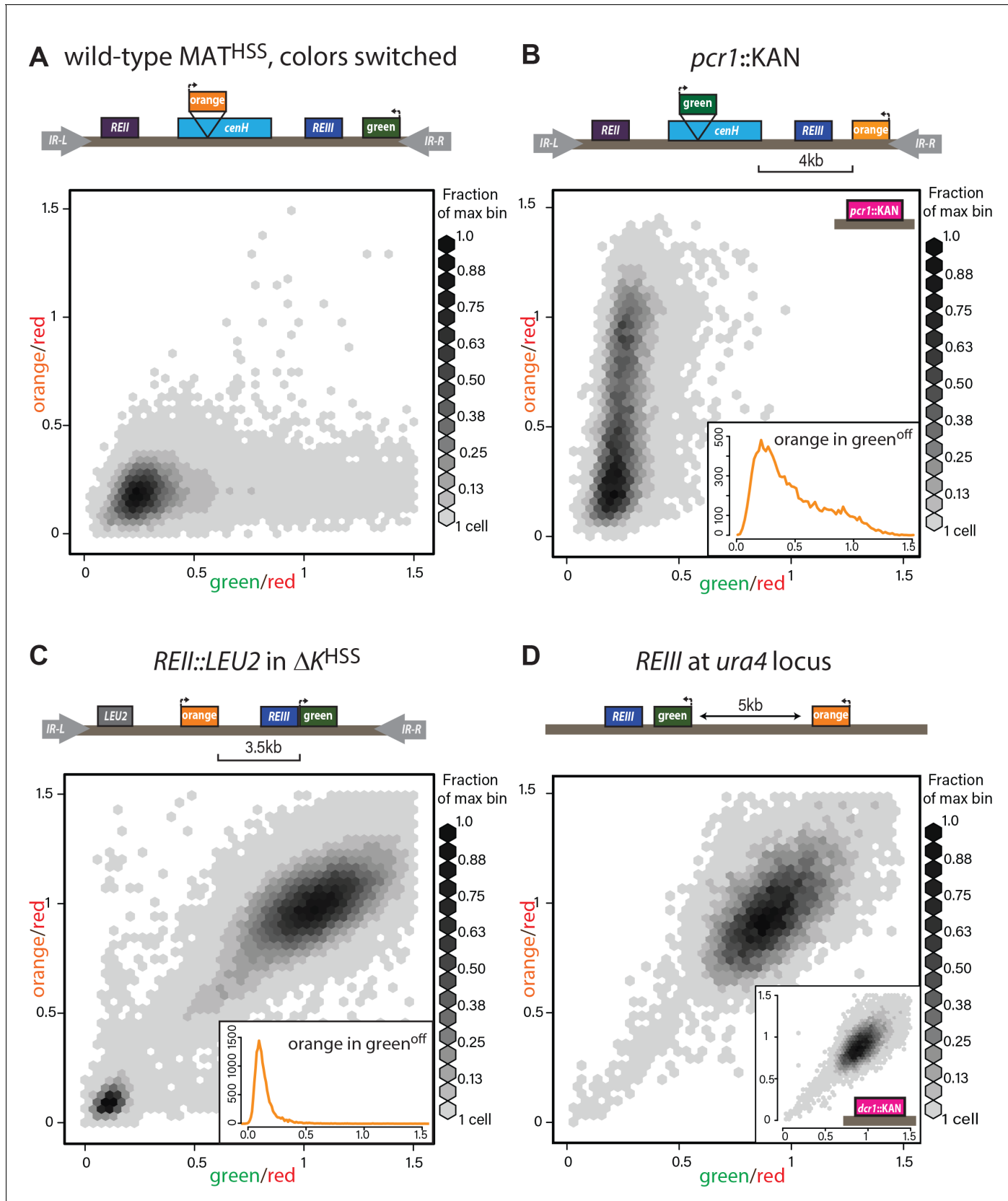


Figure 2—figure supplement 1. Heterochromatin spreading characteristics of cis-acting elements at the tightly repressed MAT locus. (A) The MAT^{HSS} documents tight repression of the wild-type MAT locus. As in **Figure 2A and B**, with ‘green’ and ‘orange’ switched. (B) Stochastic spreading with **Figure 2—figure supplement 1 continued on next page**

Figure 2—figure supplement 1 continued

intermediate states in *pcr1::KAN*. *pcr1* transcription factor was knocked-out in the PAS217 wild-type MAT^{HSS}. Plot and inset as in **Figure 2B**. (C) *REII* does not contribute to bimodal distribution seen for ΔK^{HSS} . The *REII* locus (1 kb) was replaced with the *LEU2* gene before *clr4+* was introduced by cross. (D) *REIII* is unable to establish spreading at an ectopic site. 2D density hexbin plots of *ura4::REIIIHSS^{5kb}*. Normalized green and orange are near 1.0, indicating a failure to repress both reporters. Inset: 2D density hexbin plots of *ura4::REIIIHSS^{5kb}* *dcr1::KAN*. *dcr1* was deleted to release extra heterochromatin factors from RNAi-repressed loci. No additional silencing is detected.

DOI: <https://doi.org/10.7554/eLife.32948.005>

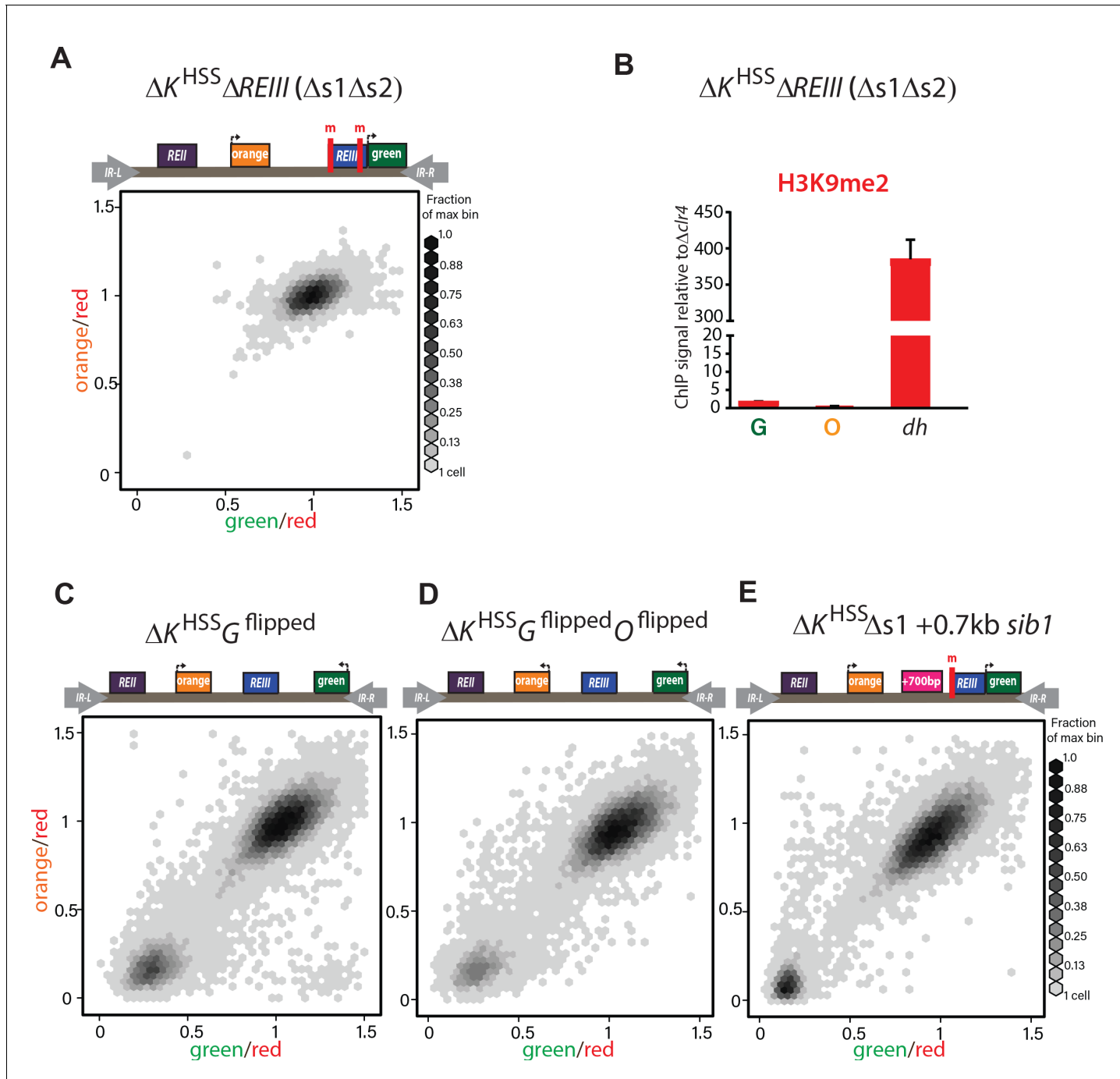


Figure 2—figure supplement 2. *REIII* is required for heterochromatin formation in ΔK^{HSS} . (A) Deletion of both Atf1/Pcr1-binding sites before introduction of *clr4+* in ΔK^{HSS} blocks gene silencing. In 34/34 strains tested (one representative shown), $\Delta K^{HSS} \Delta s1 \Delta s2$ cannot form repressed states. (B) H3K9me2 does not accumulate when both Atf1/Pcr1-binding sites are deleted in ΔK^{HSS} . H3K9me2 ChIP in $\Delta K^{HSS} \Delta s1 \Delta s2$ at 'green', 'orange' and *dh*. ($\Delta K^{HSS-OFF}$) accumulates H3K9me2 to similar extent as *dh*, **Figure 2E**). Error bars indicate standard deviation of technical replicates. (C) 'green' orientation and position does not substantially affect ΔK^{HSS} behavior. In $\Delta K^{HSS} G$ flipped, 'green' is flipped in orientation with respect to ΔK^{HSS} . (D) 'green' and 'orange' orientations do not substantially affect ΔK^{HSS} behavior. In $\Delta K^{HSS} G$ flipped O flipped, 'green' is located as in C and 'orange' is flipped in orientation with respect to ΔK^{HSS} . 'green' in (C) and (D) is 2.1 kb downstream from its location in ΔK^{HSS} now on the distal side of the *mat3m* cassette. (E) Increasing distance between *REIII* and 'orange' does not substantially affect ΔK^{HSS} behavior. The Atf1/Pcr1-binding site proximal to 'orange' was deleted ($\Delta s1$) and 700 bp of the *sib1* ORF inserted to the left of the $\Delta s1$ site. 2D-hexbin plots as in **Figure 2**.

DOI: <https://doi.org/10.7554/eLife.32948.006>

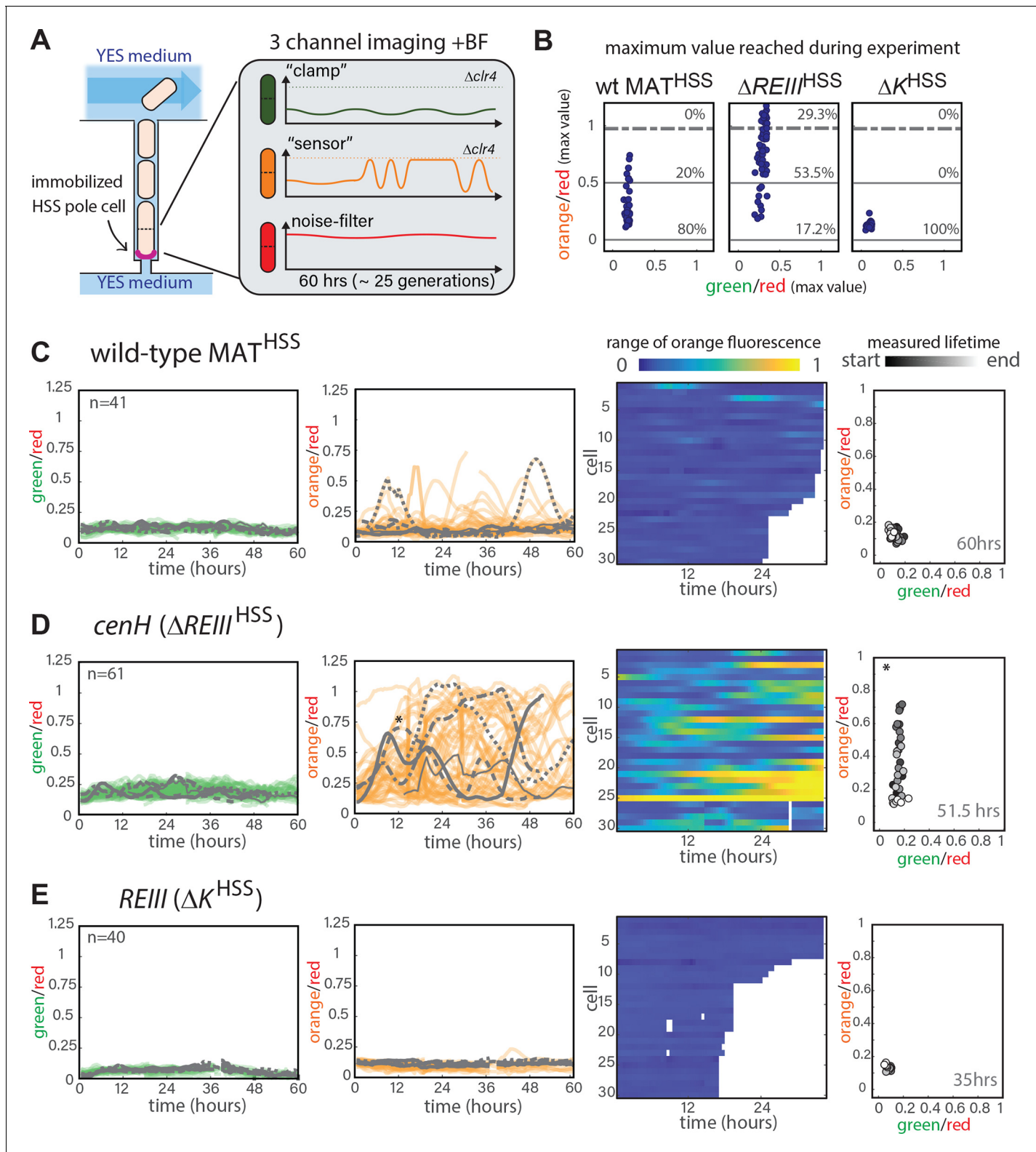


Figure 3. Single-cell analysis of nucleation and spreading using a Fission Yeast Lifespan Micro-dissector (FYLM). (A) Overview of the FYLM-based heterochromatin spreading assay. The old-pole cell is trapped at the bottom of one of hundreds of wells in the FYLM microfluidic device and is continuously imaged in brightfield (to enable cell annotation), green, orange and red channels. Hypothetical example traces are shown. (B) Maximum values attained by each nucleated cell for normalized 'orange' plotted against normalized 'green'. Solid horizontal lines correspond to $y = 0$ and $y = 1$. (C-E) Analysis of wild-type MAT^{HSS}, cenH ($\Delta REIII^{HSS}$), and REIII (ΔK^{HSS}) cells. (C) Wild-type MAT^{HSS} shows low orange fluorescence and no nucleation. (D) cenH ($\Delta REIII^{HSS}$) shows high orange fluorescence and nucleation. (E) REIII (ΔK^{HSS}) shows low orange fluorescence and no nucleation. * indicates significant difference between wild-type and mutant.

Figure 3 continued

$y = 0.5$. Dashed line corresponds to an ON cutoff determined by mean less three standard deviations for each strain's matched $\Delta clr4$ strain. Percentage of cells between each line was calculated. (C) FYLM analysis of wild-type MAT^{HSS} cells. CELL TRACES: 60 hr of normalized 'green' (left) and 'orange' (right) fluorescence in cells that maintained nucleation with the same five cells overlaid in different gray line styles in both plots. Gaps indicate loss of focus. HEATMAP: Up to 36 hr of normalized 'orange' fluorescence for 30 cells that maintained nucleation is represented from blue (0) to yellow (1). X-Y FLUORESCENCE PLOT: for one representative sample cell, plot of normalized 'green' and 'orange' fluorescence across its measured lifetime (grayscale). (D) FYLM analysis of $\Delta REII$ ^{HSS} cells as in C. The example cell in the X-Y dot plot is marked with an asterisk(*) on the orange traces (E) FYLM analysis of $\Delta K^{HSS-OFF}$ isolate, as in C., D. All cells were normalized to $\Delta clr4$ (max, 1).

DOI: <https://doi.org/10.7554/eLife.32948.007>

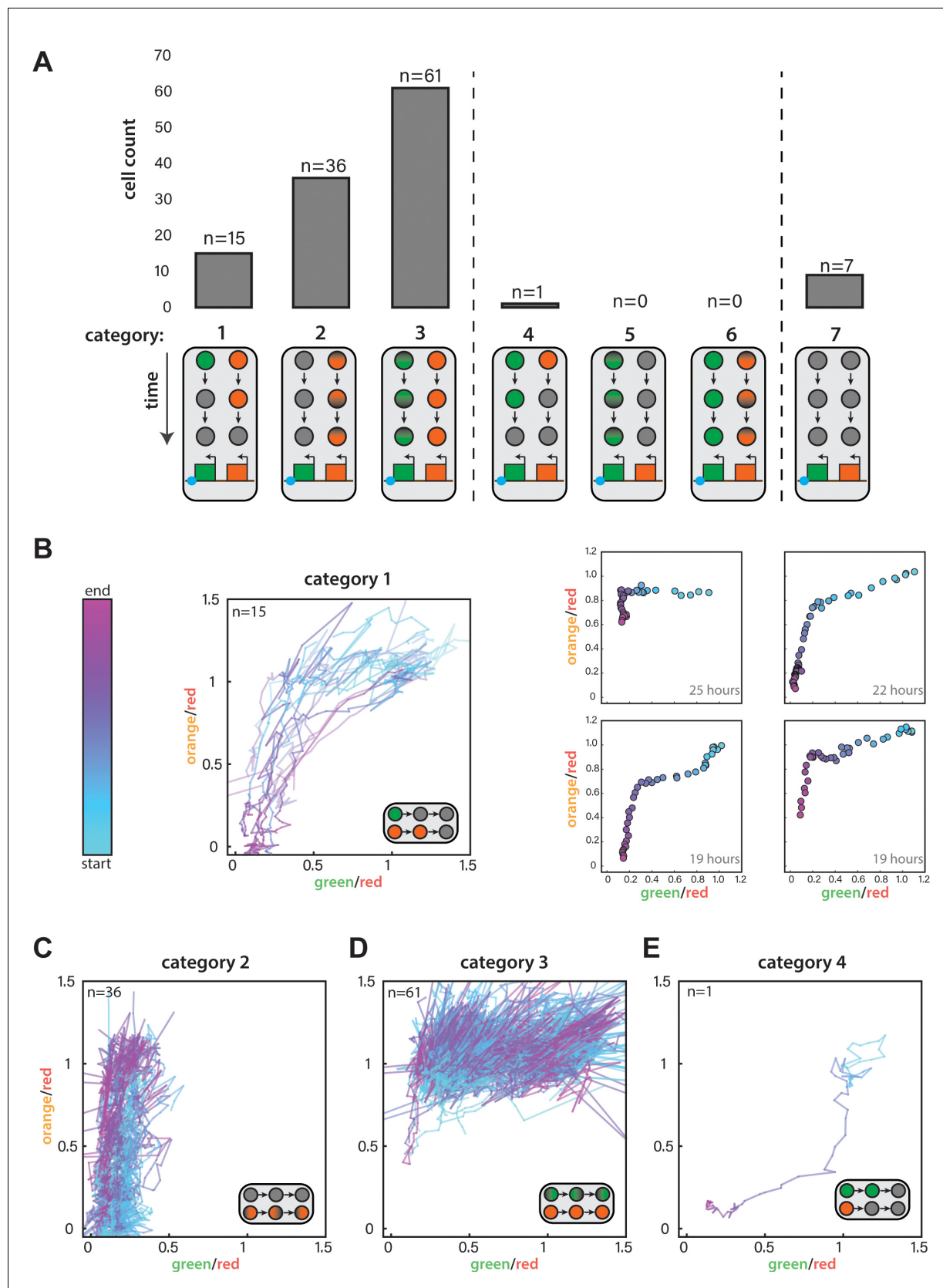


Figure 3—figure supplement 1. Single-cell analysis of nucleation and spreading using a Fission Yeast Lifespan Micro-dissector (FYLM). (A) For *ura4::dhHSS^{3kb}* FYLM experiments, counts of cells in each of seven categories. Diagrams indicate the time-dependent silencing behaviors of cells in each

Figure 3—figure supplement 1 continued

category. Categories 1–3 are consistent with proximal to distal silencing, whereas categories 4–6 are consistent with a distal to proximal silencing. (B) Time-dependent traces showing cells from Category 1 where the normalized ‘green’ and ‘orange’ values at each time point are plotted color-coded by time where blue and pink represent the start and end of the measurement, respectively. LEFT: Traces for all Category 1 cells, which begin at the start of the silencing event with both colors fully expressed and end when both colors have reached their local minimum. RIGHT: Four example cells where points represent 30-min time points colored from the start to end of the event. The duration of the time represented is indicated in the lower right corner. (C) Traces for Category 2 cells during their entire measured lifespan. (D) Traces for Category 3 cells during their entire measured lifespan. (E) Time-dependent traces for the one cell in Category 4. Lines are plotted and time is curated as in (B).

DOI: <https://doi.org/10.7554/eLife.32948.008>

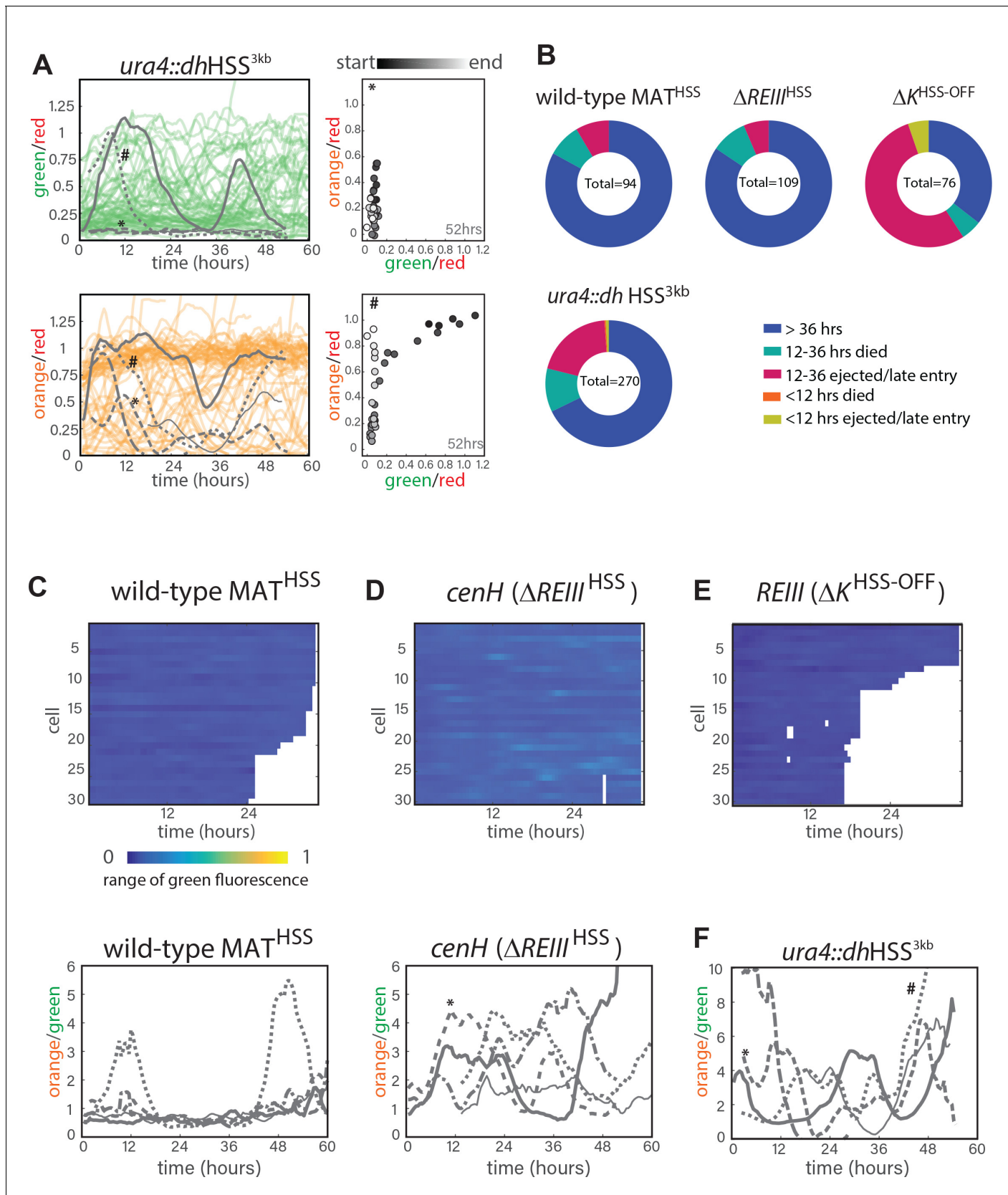


Figure 3—figure supplement 2. Single-cell analysis of nucleation and spreading using a Fission Yeast Lifespan Micro-dissector (FYLM). (A.) FYLM analysis of *ura4::dhHSS^{3kb}* cells. TOP LEFT: 60 hr of normalized 'green' fluorescence, a subset of cells are shown for clarity. five example cells are Figure 3—figure supplement 2 continued on next page

Figure 3—figure supplement 2 continued

overlaid in gray each with different line types. BOTTOM LEFT: 60 hr of normalized 'orange' fluorescence in the matching subset of cells with the same five overlaid in gray. *, # represent two example cells. RIGHT: for two representative sample cells imaged, plots of normalized 'green' and 'orange' across its measured lifetime (grayscale). The corresponding cells are marked in the orange traces on LEFT. (B) Categorization of cell longevity of all cells analyzed in the FLYM experiment. Measured lifespan ends when a cell dies or is ejected from its capture channel. (C) For wild-type MAT^{HSS} TOP: 'green' fluorescence heatmap (blue (0) to yellow (1)) for the same 30 cells as in 3C. BOTTOM: 60 hr of traces for 'orange' divided by 'green' for the five example cells indicated in 3C. (D) 'green' fluorescence heatmap and 'orange'/'green' traces for $\Delta REII^{HSS}$ as in C. (E) 'green' fluorescence heatmap ΔK^{HSS} as in C. (F) 'orange'/'green' traces for *ura4::dhHSS^{3kb}* as in C. *, # indicate the same cells as in A.

DOI: <https://doi.org/10.7554/eLife.32948.009>

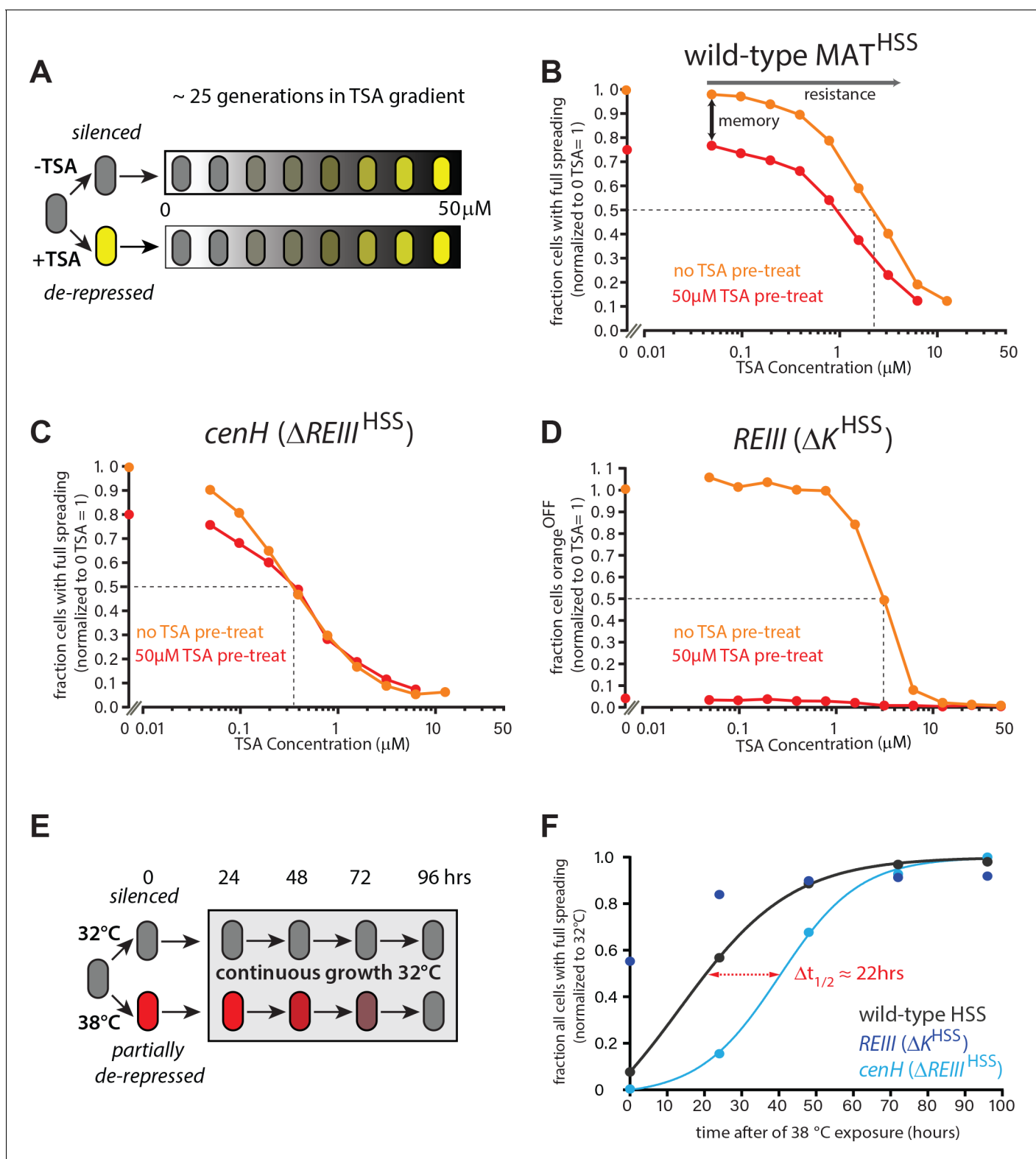


Figure 4. ncRNA-nucleated spreading exhibits weak memory and resistance in the absence of *REIII*. (A) Experimental schematic for memory and resistance measurements. Cells in log phase were treated with TSA (50 μM) for 10 generations to erase all heterochromatin (de-repressed, yellow) or kept untreated (repressed, grey). Both populations are then grown in a gradient of TSA concentration from 0 to 50 μM for 25 generations. (B) The wild-type MAT locus exhibits memory in silencing ‘orange’ throughout the TSA gradient. The fraction of ‘green’^{OFF} cells that fully silence ‘orange’ normalized to the no TSA pre-treatment, 0 μM TSA point are plotted for each TSA concentration. Red line: cell ancestrally TSA pre-treated; light orange line: cell not pre-treated. (C) The *cenH* ($\Delta REIII$)^{HSS} locus exhibits memory and resistance. (D) The *REIII* (ΔK)^{HSS} locus exhibits loss of memory and resistance. (E) Continuous growth experiments show that the transition from ‘silenced’ to ‘partially de-repressed’ occurs over 24–48 hours. (F) Spreading kinetics show that the half-time for spreading ($\Delta t_{1/2}$) is approximately 22 hours for the *REIII* (ΔK)^{HSS} locus. Figure 4 continued on next page

Figure 4 continued

orange line: cells without pre-treatment. (C) Spreading from *cenH* exhibits weak memory and low resistance. Cell populations as above. (D) ncRNA-independent spreading exhibits high resistance. The fraction of 'orange'^{OFF} for all cells is plotted, because in the TSA pre-treatment almost no 'green'^{OFF} cells can be detected. Dotted lines indicate the half-resistance points: TSA concentration at which 50% of non-pretreated cells fail to form heterochromatin at 'orange'. Memory is the difference between orange and red lines. One of two full biological repeats of the experiment is shown. (E) Experimental schematic for heat stress and recovery. Cells were grown at either 32 or 38°C for 10 generations and strains subsequently grown continuously for 96 hr at 32°C. (F) The fraction of cells with full spreading ('green'^{OFF} and 'orange'^{OFF}) after 38°C exposure and recovery normalized to the fraction of cells with full spreading at 32°C for each strain is plotted over time. For wild-type MAT^{HSS} and *ΔREII*^{HSS} strains, we fit a simple sigmoidal dose response curve and determined a $t_{1/2}$ value. The difference in $t_{1/2}$ values or $\Delta t_{1/2}$ is ~22 hr or ~9–10 generations.

DOI: <https://doi.org/10.7554/eLife.32948.015>

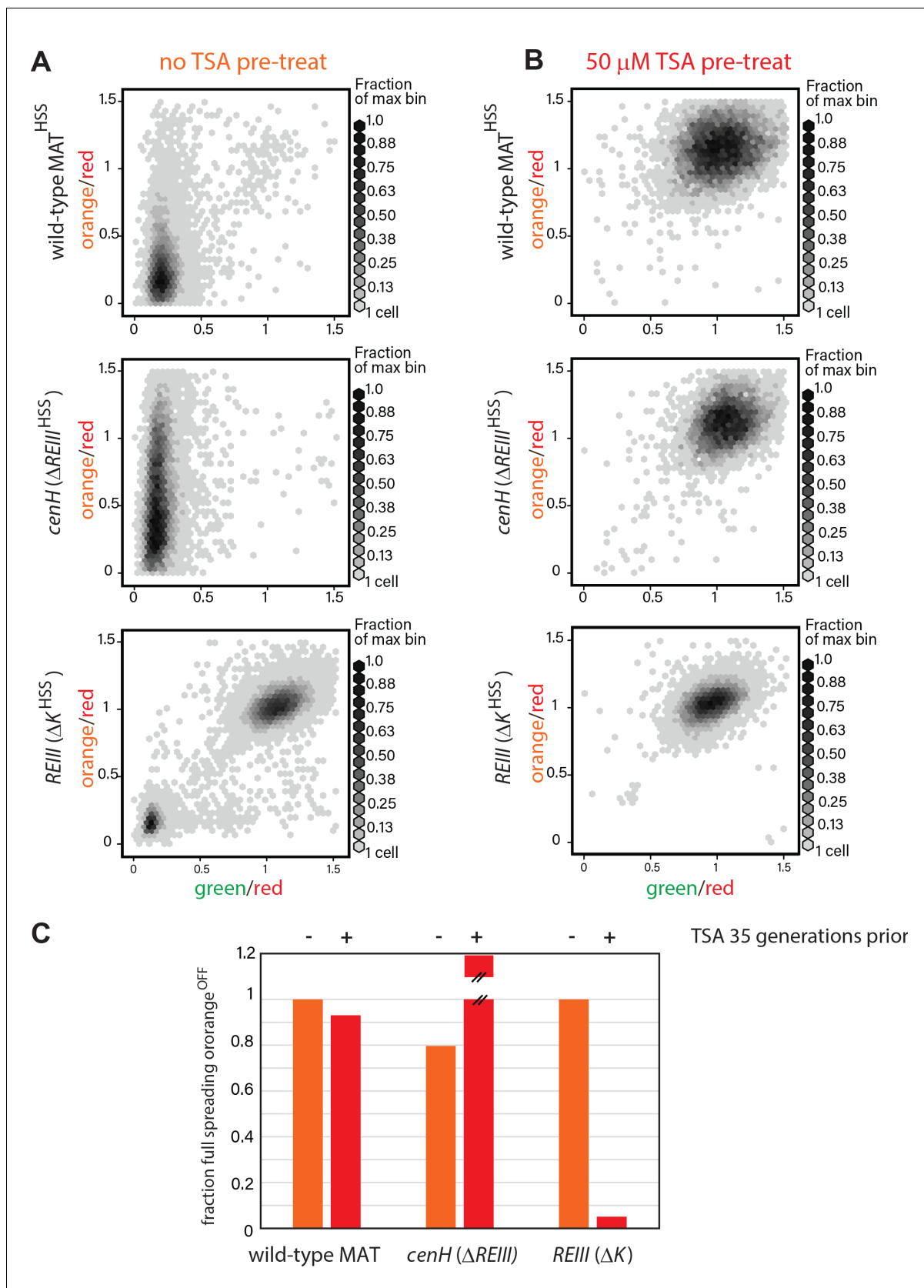


Figure 4—figure supplement 1. heterochromatin behaviors during TSA treatment and after 35 generations. (A) 2D density hexbin plots of wild-type MAT^{HSS}, Δ REIII^{HSS}, and Δ K^{HSS} strains grown 10 generations without TSA. (B) 2D density hexbin plots of wild-type MAT locus^{HSS}, Δ REIII^{HSS}, and Δ K^{HSS} strains grown 10 generations after 35 generations of TSA treatment. (C) Bar chart showing the fraction of full spreading orange OFF for each strain under different conditions. The y-axis ranges from 0 to 1.2. The x-axis categories are wild-type MAT, cenH (Δ REIII), and REIII (Δ K). For each category, there are two bars: a blue bar for '-' and a red bar for '+'. Error bars are shown for the red bars.

Figure 4—figure supplement 1 continued

strains grown 10 generations in 50 μM TSA. The density distributions are near 1.0 in all strains indicating complete erasure of heterochromatin. (C) History dependence at 35 generations after pretreatments. The fraction of cells with full spreading (wild-type MAT and ΔREII) or fraction of cells with orange^{OFF} (ΔK) normalized to the highest value for ancestrally untreated cells (=1) is shown for the 0 μM TSA point. TSA pretreated cells for $\Delta\text{REII}^{\text{HSS}}$ show higher repression than untreated cells. We interpret this to indicate experimental variations in silencing in the absence of memory. This is because for all other circumstances, TSA treatment results in reduced spreading, including for $\Delta\text{REII}^{\text{HSS}}$ at 25 generations post-treatment.

DOI: <https://doi.org/10.7554/eLife.32948.016>

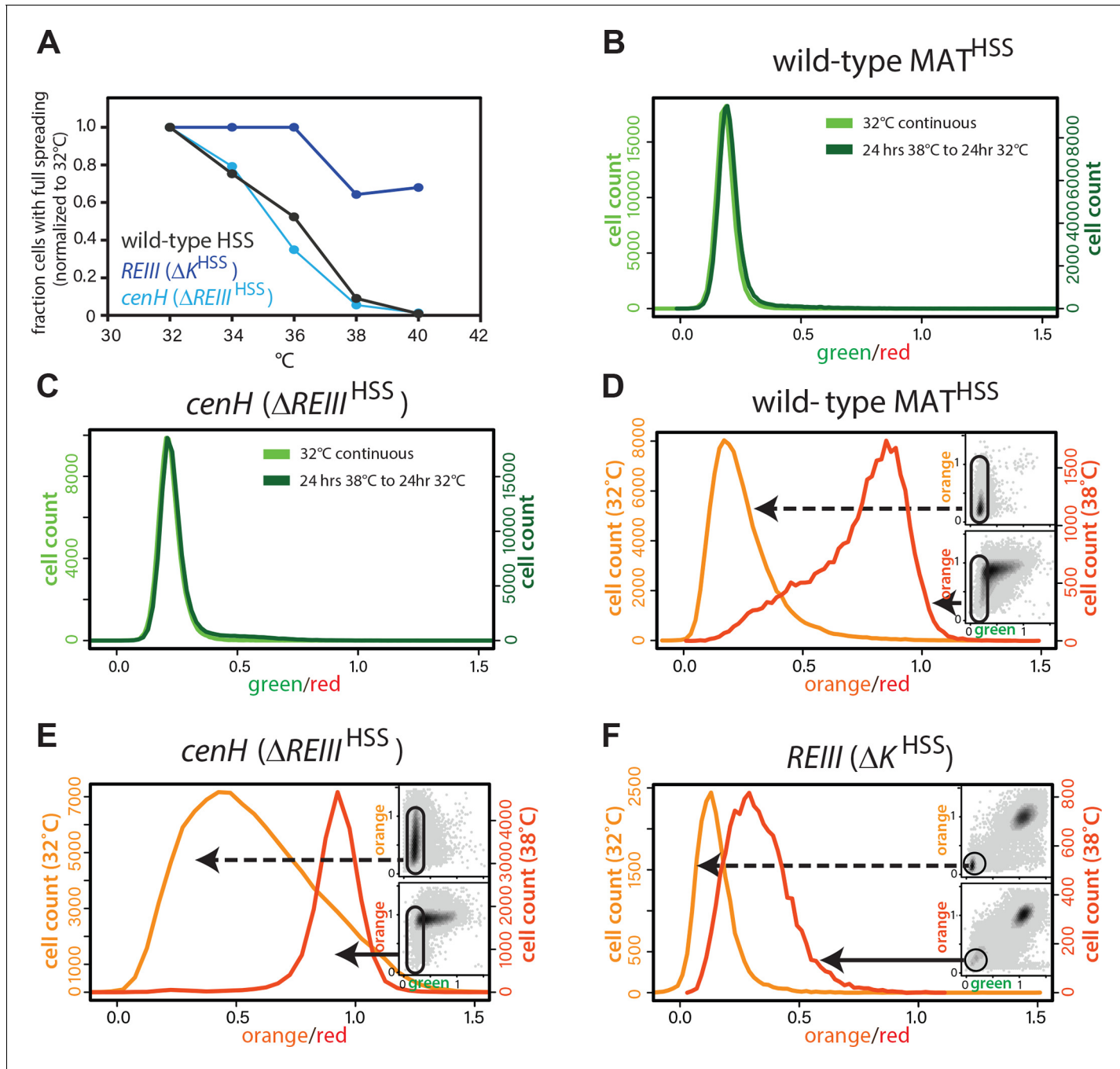


Figure 4—figure supplement 2. Behavior of MAT heterochromatin at elevated temperature. (A) The resistance of the heterochromatin state from 32°C to 40°C in wild-type MAT^{HSS}, ΔK^{HSS} , and $\Delta REIII^{HSS}$. The fraction of cells that fully repress both 'orange' and 'green' (full spreading) at each temperature is plotted normalized to the given strains value at 32°C. (B and C) nucleation is recovered within 24 hr at 32°C. 1-D histogram showing the distribution of green fluorescence in wild-type MAT locus^{HSS} (B) or $\Delta REIII^{HSS}$ (C) cells grown either for 48 hr continuously at 32°C (left y-axis, light green) or heat stressed for 24 hr at 38°C followed by 24 hr growth at 32°C (right y-axis, dark green). (D–F) Histograms of 'red'-normalized 'orange' fluorescence distribution in 'green'^{OFF} cells are shown for cells grown at both 32°C (light orange) and 38°C (dark orange). Insets: 2D density hexbin plots, 'green'^{OFF} cells are schematically circled. (C–E) represent t = 0 in **Figure 4F**.

DOI: <https://doi.org/10.7554/eLife.32948.017>

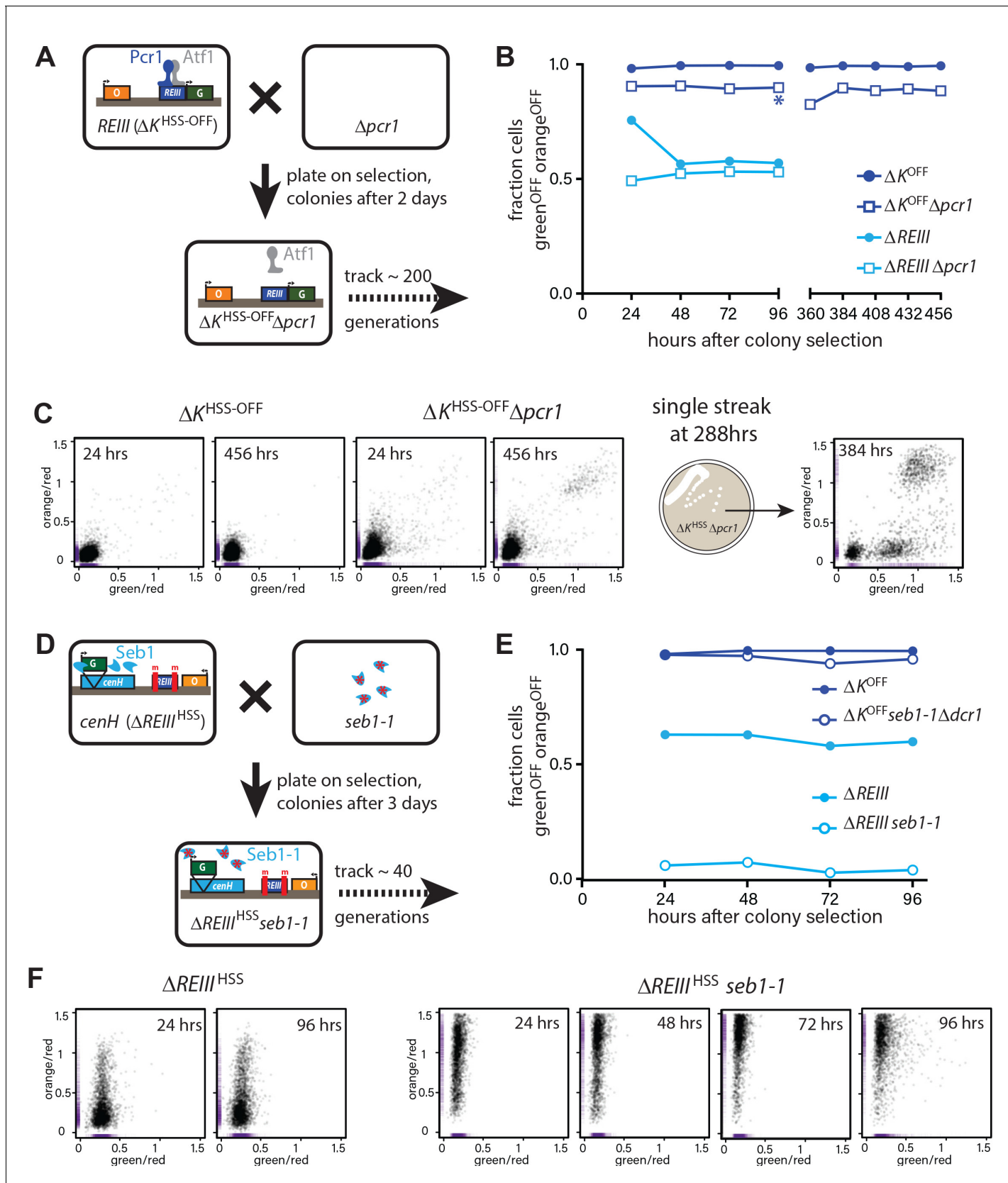


Figure 5. Differential inheritance of ncRNA-dependent and independent spreading in the absence of nucleation factors. (A) Scheme for removal of Pcr1 (REIII binding factor) in the ΔK^{HSS} strain OFF isolate ($\Delta K^{HSS-OFF}$). Progeny of the cross was selected for $\Delta K^{HSS-OFF} \Delta pcr1$ genotype and identifiable

Figure 5 continued on next page

Figure 5 continued

colonies immediately grown for cytometry, and passaged for 456 hr. (B) Stable inheritance of repression in $\Delta K^{HSS-OFF}\Delta pcr1$. $\Delta K^{HSS-OFF}\Delta pcr1$ or $\Delta K^{HSS-OFF}$ cells (dark blue lines) where analyzed by flow cytometry over consecutive days, the break indicating passaging without analysis. $\Delta pcr1$ had no significant effect on $\Delta REIII^{HSS}$ (light blue lines). (C) LEFT: scatter plots with partial point transparency of $\Delta K^{HSS-OFF}$ or $\Delta K^{HSS-OFF}\Delta pcr1$ early and late in the time course. RIGHT: In the middle of the time course (asterisk in (B)), $\Delta K^{HSS-OFF}\Delta pcr1$ were struck for single colonies. The scatter plots for one of the isolates is shown. (D) Scheme for removal of functional Seb1 in $\Delta REIII^{HSS}$ strain. Selection and growth as in A., total passaging time 96 hr. (E) Weak inheritance of repression in $\Delta REIII^{HSS}seb1-1$ (light blue lines). Analysis as above, total time course 96 hr. Removal of both Seb1 and RNAi pathways ($\Delta K^{HSS-OFF}seb1-1\Delta pcr1$) does not affect maintenance of silencing (dark blue lines). (F) Scatter plots of $\Delta REIII^{HSS}$ at 24 and 96 hr and through the entire time course for $\Delta REIII^{HSS}seb1-1$. In these scatter plots, X and Y values of each cell are represented by purple dashes along the corresponding axis.

DOI: <https://doi.org/10.7554/eLife.32948.018>

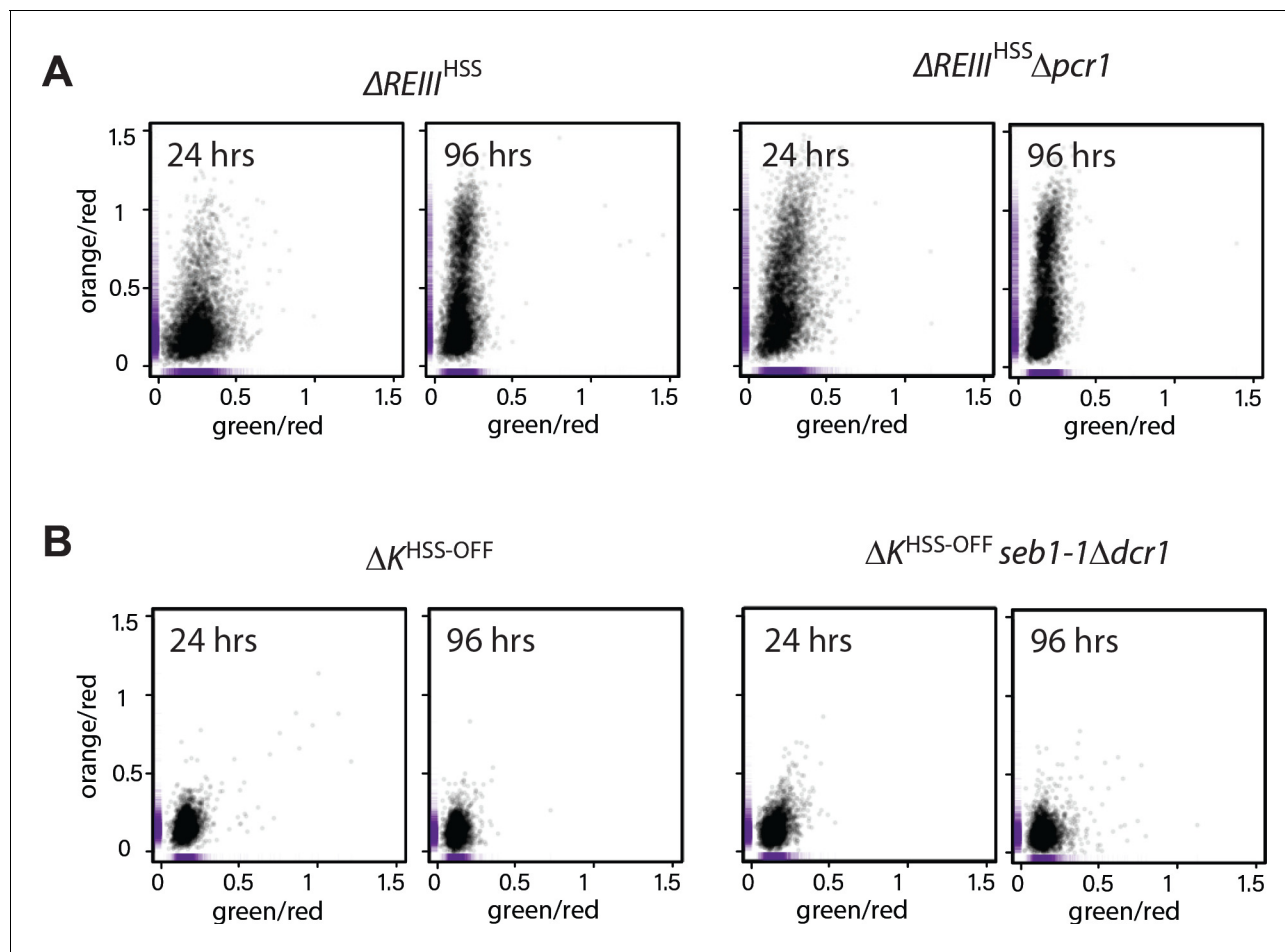


Figure 5—figure supplement 1. trans-factor mutants do not substantially affect spreading when their cognate *cis*-acting element is inactivated. (A) Scatter plots of $\Delta REIII^{HSS}$ and $\Delta REIII^{HSS} \Delta pcr1$ at 24 and 96 hr. (B) Scatter plots of ΔK^{HSS} and $\Delta K^{HSS} seb1-1 \Delta dcr1$ at 24 and 96 hr. The *seb1-1* and $\Delta dcr1$ double mutant should abolish all RNA-dependent nucleation (Marina et al., 2013). The X and Y values of each cell are represented by purple dashes along the axis.

DOI: <https://doi.org/10.7554/eLife.32948.019>

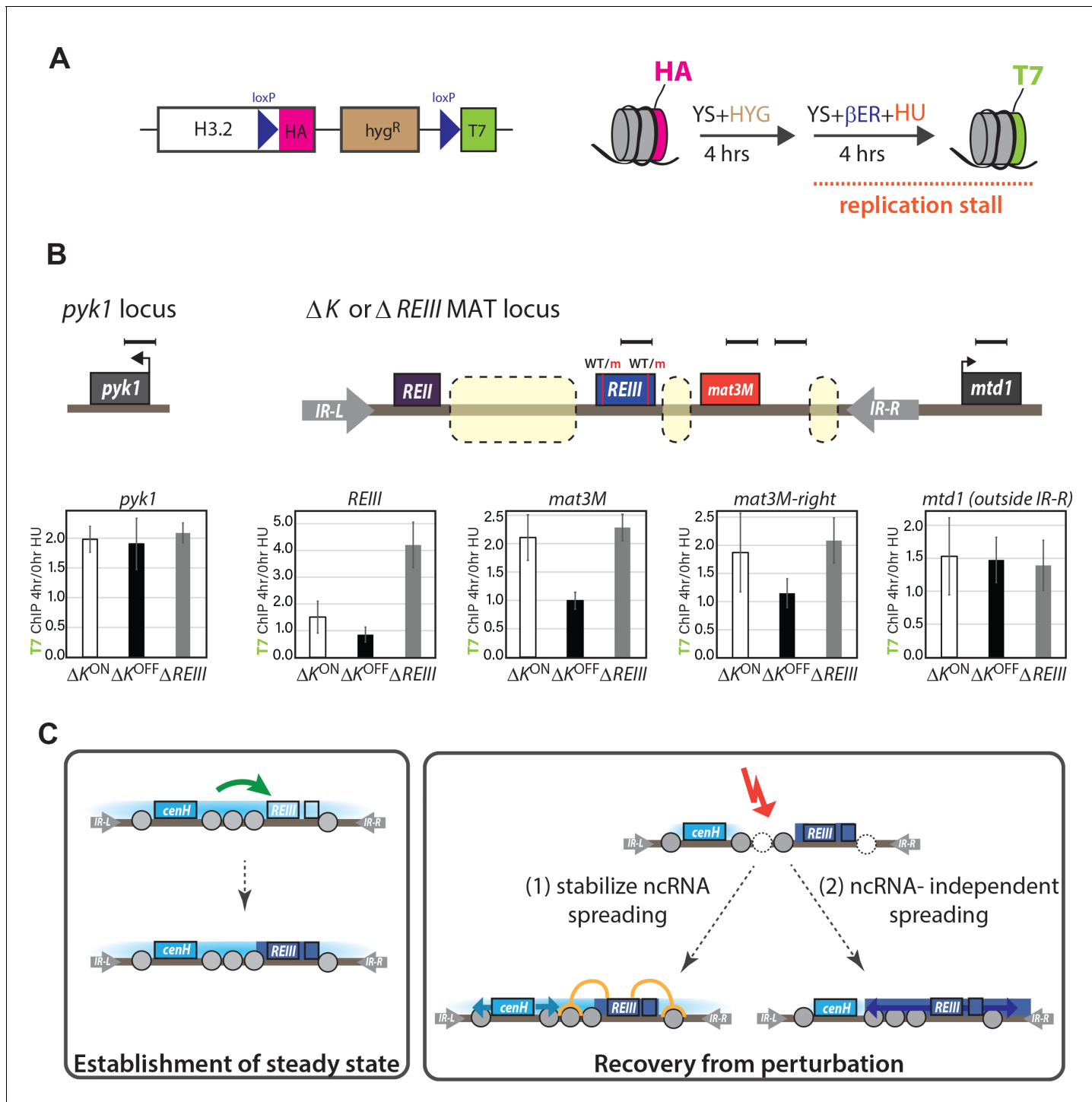


Figure 6. Histone turnover correlates with epigenetic stability in ncRNA-dependent and *REIII*-dependent heterochromatin. (A) LEFT: Overview of the LEITE system for histone 3.2. Cre recombinase allows tag exchange from HA to T7. RIGHT: experimental scheme for detecting replication-independent H3 turnover. Cells were grown to log phase and then grown for 4 hr in the presence of β -estradiol and 15 mM hydroxyurea. (B) Enrichment for H3-T7 at indicated loci in ΔK^{HSS-ON} , $\Delta K^{HSS-OFF}$ or $\Delta REIII^{HSS}$ strain. TOP: Location of amplicons for T7-ChIP indicated by bars. Dashed boxes in MAT indicated regions of genomic difference between ΔK^{HSS} and $\Delta REIII^{HSS}$. WT and m for *REIII* indicate presence or deletion of Atf1/Pcr1-binding sites, respectively. BOTTOM: Enrichment of T7 tag by ChIP at 4 hr in HU over 0 hr for indicated strains. one indicates no enrichment over 0 hr. Error bars indicate standard deviation of technical replicates. (C) Model for collaboration of *cenH* and *REIII* in establishing and maintaining the high fidelity MAT locus. (LEFT) During initial establishment, *cenH* heterochromatin raises the nucleation frequency at *REIII* (green arrow). A box right of *REIII* represents a putative additional nucleation element. (RIGHT) Labile *cenH*-nucleated spreading is disrupted, in part by de-stabilized nucleosomes, in a environmental

Figure 6 continued on next page

Figure 6 continued

perturbation or a stochastic event. *REIII* promotes reestablishment of the initial state by repressing histone turnover, limiting nucleosome loss (orange) and thus aiding spreading from *cenH* (light blue arrows, (1)), or promoting heterochromatin spreading from surrounding elements (dark blue arrows, (2)).

DOI: <https://doi.org/10.7554/eLife.32948.020>

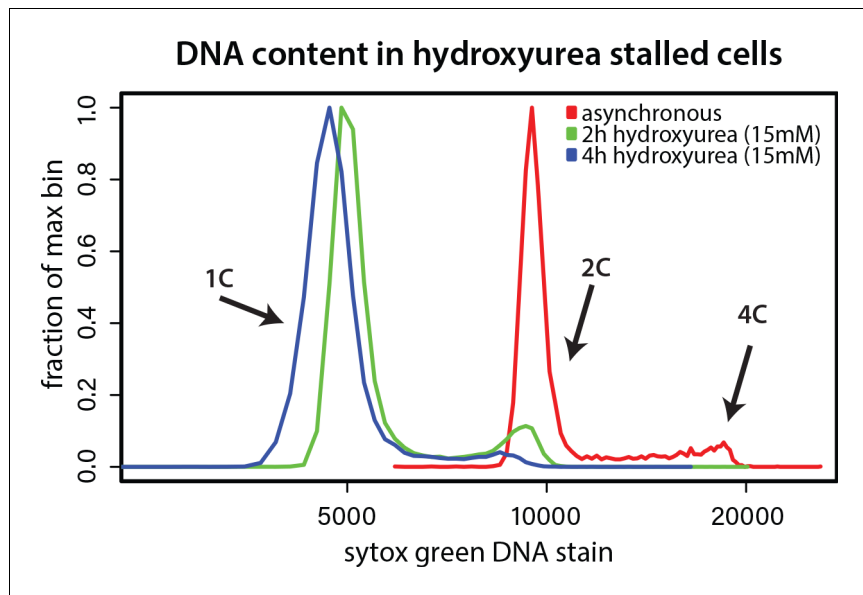


Figure 6—figure supplement 1. Hydroxyurea induced cell cycle arrest. Cells were grown without (asynchronous) or with 15 mM hydroxyurea for 2 or 4 hr and DNA content was determined by Sytox green staining and flow cytometry. Hydroxyurea treatment stalls cells in early S phase, evident from loss of 2 and 4C peaks.

DOI: <https://doi.org/10.7554/eLife.32948.021>